Structural study of the oxidation process and stability of $NbO_x N_y$ coatings

J.M. Chappé [a], P. Carvalho [a], A.V. Machado [a], F. Vaz [a], E. Alves [b,*], N.P. Barradas [b], M. Fenker [c], H. Kappl [c]

[a] Departamento de Física, Universidade do Minho, 4800-058 Guimarães, Portugal

[b] Departamento de Física, Instituto Tecnológico Nuclear, E.N. 10, 2686-953 Sacavém, Portugal

[c] FEM, Departmento POT-MPh, Katharinenstrasse 17, D-73525 Schwäbisch Gmünd, Germany

Keywords:

$NbO_x N_y$ coatings
Reactive sputtering
Oxidation
Thermal stability

Abstract

In the present work, we study the oxidation behaviour of NbON multilayer films. The films were deposited by DC magnetron sputtering with a reactive gas pulsing process. The nitrogen flow was kept constant and the oxygen flow was pulsed. Pulse durations of 10 s produced multilayered coatings with a period of $\lambda = 10$ nm. Three different films with increasing duty cycles have been deposited.

Rutherford backscattering spectroscopy (RBS) was used to study the chemical composition variations at different annealing temperatures (as-deposited, 400°C, 500°C and 600°C) combined with X-ray diffraction (XRD) to identify the crystalline phases formed. At 400°C, for all films a very thin layer starts to form at the surface with enhanced O concentration. The composition of the deeper part of the samples remains unchanged. At 500°C, the oxide scale grows, encompassing about half the film thickness. At 600°C, the process is finished and a single layer is formed with reduced Nb and increased O concentration. Fourier-transformation infrared spectroscopy (FTIR) results

confirmed the increase of this surface oxidation, while XRD revealed that crystallization of Nb_2O_5 occurs at 600°C.

Introduction

The number of publications per year in the field of oxynitrides increased significantly in the last 5 years, showing the growing interest and importance of this class of coating material. The possibility to control the film properties by playing with the oxygen-to-nitrogen ratio makes this type of materials highly interesting for a large number of applications. The field of applications is wide: decorative coatings [1], solar absorbers [2,3], gate dielectrics in semiconductor devices [4], biocompatible materials (TiNbON) [5], optical waveguides (SiON, NbON) [6], etc. Apart from patents, only one reference was found about NbON thin films applied as a CrON/ NbON multilayer topcoat to increase the corrosion resistance of CrN/NbN-coated high speed steel [7]. As bulk material porous NbON is discussed as catalytic active material [8,9].

In previous studies of the $Nb-O-N$ system [10] we have reported on pulsed power reactive magnetron sputtering of Nb , $Nb-O$ and $Nb-O-N$ thin films with respect to deposition conditions, chemical composition, morphology, crystallographic structure and hardness as well as the corrosion and degradation behaviour of $Nb-O-N$ coatings. Although the results indicate that niobium nitride and oxynitrides have a good thermal stability and reveal a considerable multifunctional character [11,12], they

are expected to oxidize rapidly when exposed to oxygen or air. In the literature it is assumed that diffusion of oxygen in Nb_2O_5 occurs - presumably as a molecule and not as an ion - along the relatively open channels between the $Nb-O$ octahedron [13]. However, for the oxynitride compound ($Nb-O-N$) the oxidation behaviour is unknown and will play a crucial role for the potential applications of these coatings in high temperature environments. The formation of stable oxide layers on the coating surface, acting as oxygen diffusion barriers (like e.g. alumina or SiO_2), or on the contrary, the formation of delaminating oxide scales, due to the development of substantial compressive stresses, is a question that this work will try to answer. For this issue, the composition of the oxide layer formed on top of the coatings and the structural changes that it may induce are two of the most important features that will deserve detailed analysis in this work. However, one should keep in mind that this behaviour is strongly dependent on the chemical composition of the as-deposited films and, not less important, on the chemical composition of the oxide layers formed during the oxidation.

In order to gain better understanding on the role of coating structure and chemical composition in the oxidation mechanisms, the present paper reports on in-air oxidation resistance experiments of reactively gas-pulsed $Nb-O-N$ coatings, prepared with three different pulsing conditions. The interpretation of the results for the as-deposited samples and after annealing, provide information on the compositional changes induced by the oxidation process, allowing the study of the interaction of oxygen with the niobium oxynitrides at high temperatures and the influence of oxidation temperatures on the oxidation mechanisms.

Experimental details

$Nb-O-N$ coatings were deposited on (100) silicon substrates, by DC reactive magnetron sputtering in a lab-sized vacuum system (Leybold LH Z400). The base pressure in the chamber was lower than 6×10^{-4} Pa. Prior to the depositions the target and the substrates were sputter cleaned in pure Ar atmosphere. The depositions were performed without additional substrate heating or rotation. For the thin film deposition a metallic niobium target (purity 99.8%) was sputtered in an $Ar/O_2/N_2$ atmosphere by a reactive gas pulsing process. Films with different oxygen contents were deposited. The nitrogen flow q_{N_2} was kept constant at 2.9 sccm , whereas the oxygen flow q_{O_2} was pulsed between a minimum and a maximum flow of 0.5 sccm and 4.2 sccm , respectively. A mounting triangle was used as the pulse shape for the oxygen gas flow. Pulse durations (T) of 10 s and duty cycles $\alpha = t_{ON}/T$ of 0.3,0.6 and 0.9 were chosen (t_{ON} = injection time of oxygen). The average target current density was kept constant at 100 A m^{-2}.

The thermal oxidation of the samples was performed in a furnace, flushed with air for temperatures ranging from 400 to 600°C and an annealing time of one hour. The different thermal annealings were carried out on identical samples deposited in the same batch, and then removed from the furnace and left to cool in surrounding air. The atomic compositions of the as deposited samples and the depth profiles of the chemical concentration after annealing were measured by RBS, performed with $^1H^+$beam with energy of 1.4 MeV . A scattering angle of 140° (standard detector, IBM geometry) was used, with target tilt angles of 0° and 30°. The data were analysed with the NDF software using the ^{14}N and ^{16}O cross sections given in [14]. The results are given in at. % for the concentrations and in 1×10^{15}at/cm^2 for the thickness. These are areal density values that can be converted to real thickness values if the density of the films is known.

Infrared spectra were obtained in transmission mode on a Fourier transformed infrared (FTIR) Perkin Elmer 1600 spectrometer from 400 to 4000 cm^{-1}, using unpolarized light, with a resolution of 1 cm^{-1}. The crystallographic structure of as-deposited and annealed samples was investigated by X-ray diffraction (XRD), using a Philips PW 1710 apparatus in normal $\theta - 2\theta$ geometry (BraggBrentano). Monochromatic $CuK\alpha$ radiation ($\lambda =$ 0.15406 nm) was used.

Results and discussion

As-deposited samples

The three different as-deposited samples had a similar coating thickness of about 2μ m. Despite the short pulse durations of 10 s for oxygen, during the reactive gas pulsing process multilayered coatings with a bi-layer period of $\lambda = 10$ nm have been produced [16]. In terms of specific composition variations, it is worth to mention that in spite of the large variation in the duty cycle α, only small variations were observed in the coatings composition. Fig. 1 shows the as-deposited concentration variations for the three coatings as a function of the duty cycle, determined from the RBS data using the procedure outlined in the next section.

As expected, the oxygen increases with increasing duty cycle, consistent with the increased time while the oxygen pulse is on. Moreover, this increase is followed by a decrease of both niobium and nitrogen contents. Beyond these variation tendencies, Fig. 1

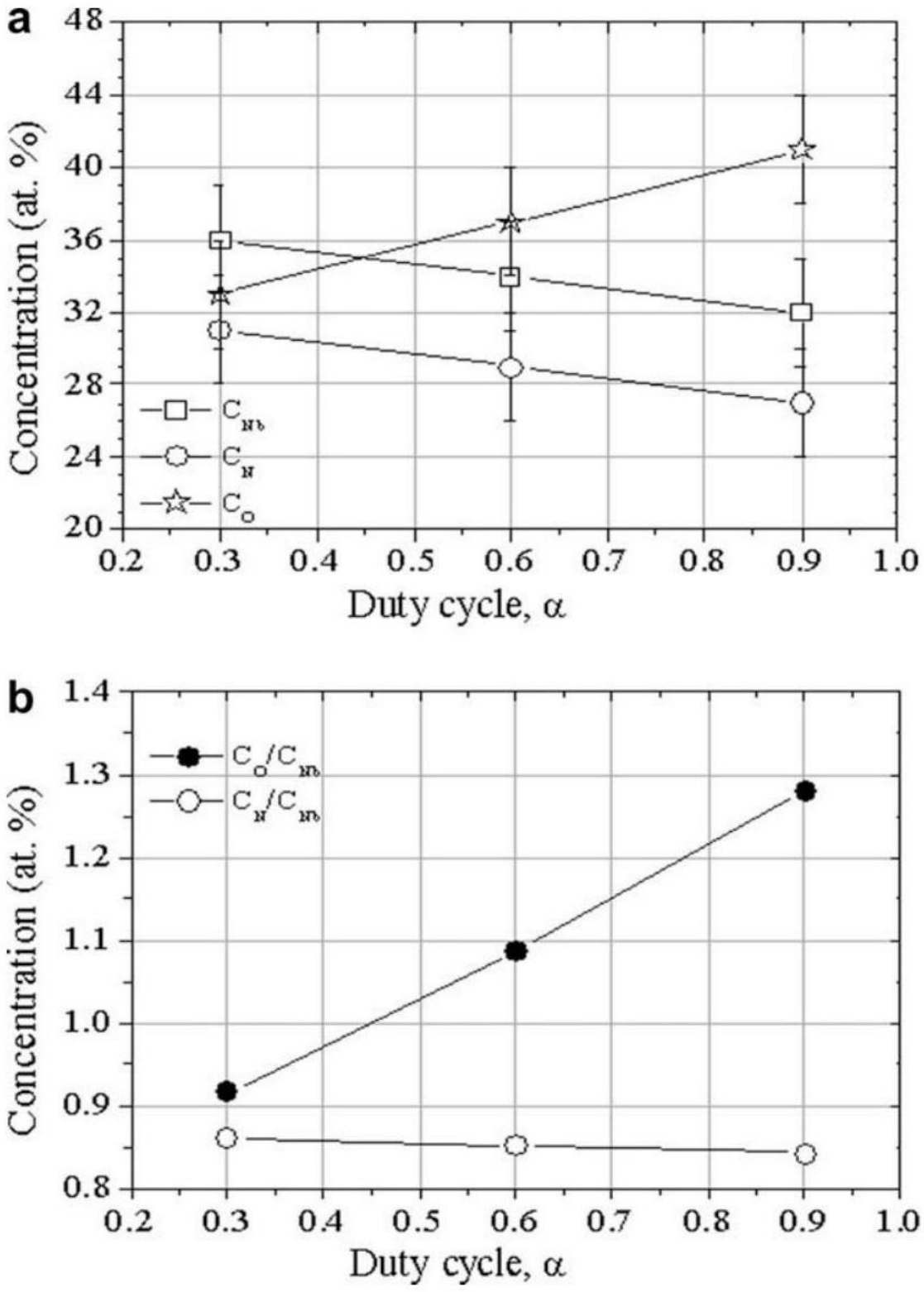

Fig. 1. Variation of (a) film's elemental concentration and (b) concentration ratios; as a function of duty cycle. Due to the RBS resolution limits, the atomic concentration of each element is plotted in (a) within an error margin of about 3at.% (but not on the

correspondent concentration ratios). also shows that the atomic ratio C_N/C_{Nb} is approximately constant, but the ratio C_O/C_{Nb} increases about 40% from ~ 0.9 to about 1.3.

As just mentioned, recent investigations by transmission electron microscopy (TEM) showed that these NbON coatings have a multilayered nanostructure with a bi-layer period of $\lambda = 10$ nm due to RGPP [15]. During the OFF-period ($t_{OFF} = T - t_{ON}$) NbN crystallites are formed in an amorphous NbON matrix, despite the fact that the pulsing times t_{OFF} and t_{ON} were very short and the oxygen flow during t_{OFF} was not completely zero. From thermodynamic data for niobium oxides and nitrides one might conclude that only niobium oxide phases are formed during t_{OFF} (NbO: $\Delta H_f = -406$ to -423 kJ/mol, NbO_2: $\Delta H_f = -791$ to -825 kJ/mol, Nb_2O_5: $\Delta H_f = -1905$ kJ/mol, Nb_2 N: $\Delta H_f = -255$ kJ/mol and NbN: $\Delta H_f = -239$ kJ/mol [12]. But it seems that the oxygen content is low enough for the formation of small NbN crystallites. The layer during the t_{ON} pulse was found to be a completely amorphous NbON layer.

In order to get some more information on the microstructure of the as-deposited films, X-ray diffraction (XRD) experiments and infrared spectra (FTIR) were combined. The XRD results were not conclusive, revealing very broad peaks in the region $2\theta \sim 30 - 35°$ (see bottom of Fig. 7), which do not allow an accurate evaluation of the phases that might be formed [12]. The formation of amorphous phases might be the most plausible conclusion for this type of behaviour. On this particular FTIR experiments give some help as it is evidenced in the spectra presented in Fig. 2. The figure shows the transmission FTIR spectra from 500 to 4000 cm^{-1} for the coatings with the three different duty cycles, revealing some

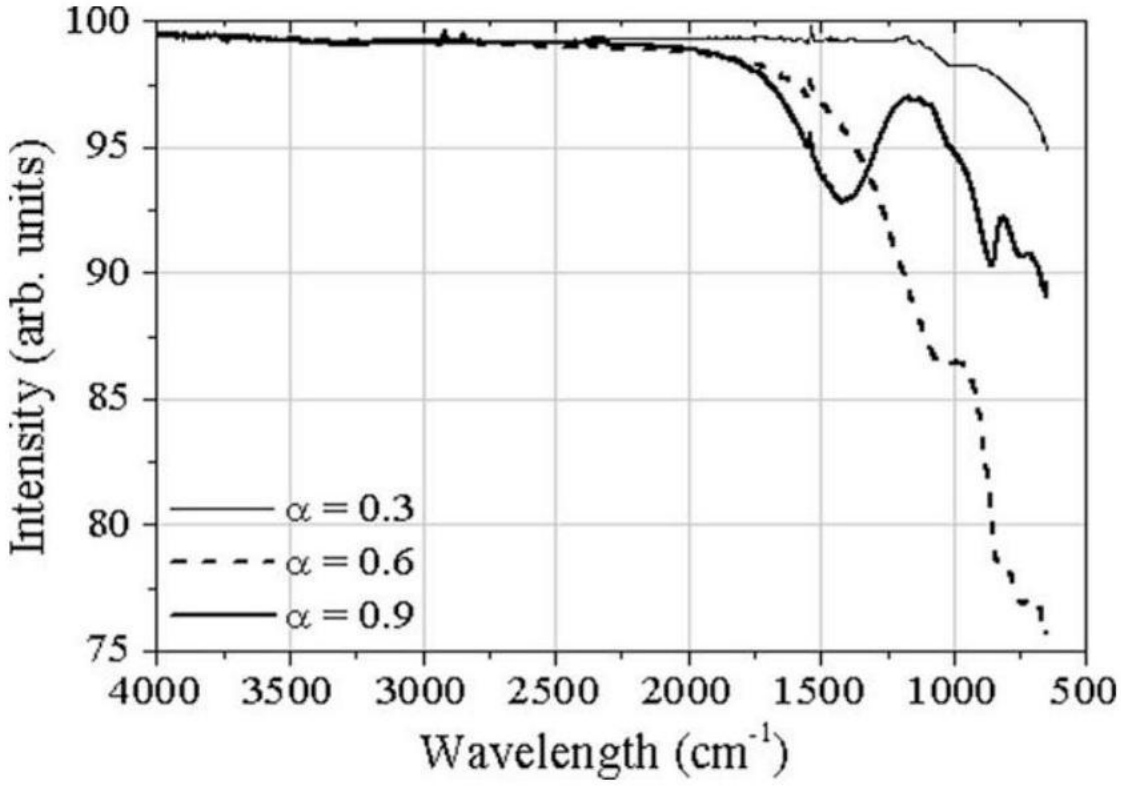

Fig. 2. Infrared transmittance spectra of niobium oxynitride thin films with duty cycles of 0.3, 0.6 and 0.9.

changes within the three different coatings that were analysed. These changes appear as a consequence of any static and/or dynamic change in the structure of the films that should, in principle, lead to a variation in the phonon behaviour, and thus the analysis of the wave-number, intensity and line width evolution of the whole spectra as a function of duty cycle is expected to give insight into the films particular arrangements. Moreover, in this kind of mixed systems, the spectra are the consequence of both shortand long-range ordered regions and chemically ordered regions. Then, the selection rules are relaxed because of the disorder, offcenter atomic shifts, presence of chemically ordered regions and/ or local symmetry and an assignment of each mode becomes highly complex.

In terms of a very specific analysis, it is clear that for the lowest duty cycle, the spectrum is related to the formation of NbN [16], where no clear band is present. As the films duty cycle increases, and consequently changing the films particular composition combinations as illustrated in Fig. 1, discontinuous changes as well as

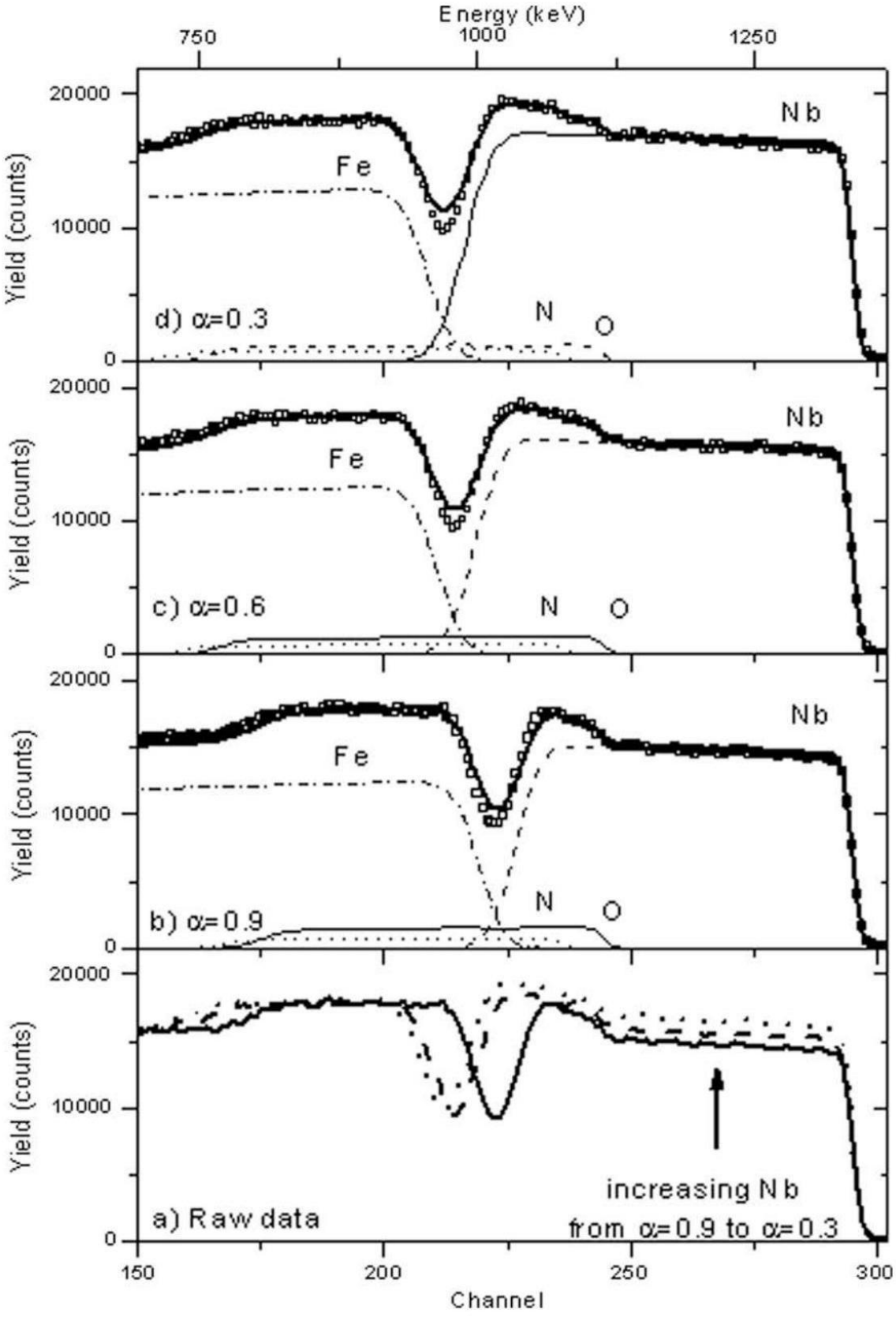
Energy (keV)
750
1000
1250
Yield (counts)
20000
10000
0
Nb
Fe
N
O
d) α=0.3
c) α=0.6
b) α=0.9
a) Raw data
increasing Nb
from α=0.9 to α=0.3
150
200
250
300
Channel

Fig. 3. RBS spectra for the as grown NbON layers: (a), and the simulation results of the layers grown with $\alpha = 0.9$ (b), $\alpha = 0.6$ (c) and $\alpha = 0.3$ (d).
smooth and continuous ones are expected to be detected in the infrared spectra. The transmission FTIR spectrum for the highest duty cycle ($\alpha = 0.9$) has a peak at 850 cm^{-1} attributed to the $Nb - O - Nb$ stretching vibrations, which are characteristic of Nb_2O_5 compounds [17,18]. An additional peak appears in the region between 1600 and 1350 cm^{-1}. This peak can be attributed to the carbon containing groups incorporated in the film structure. As indicated by Szymanowski et al. [19], three possible configurations of carbon bonds may be assigned to the peaks in this region, namely the chelating and bridging connections of the COO group with metal atoms. This can be interpreted as resulting from some film's surface contamination layer, formed after the film removal from the deposition system.

Between these two different types of films, the film prepared with $\alpha = 0.6$ reveals signals that may be indexed as a mixture of both NbN -type film and the Nb_2O_5-type film. FTIR spectrum does not have clear peaks but has shoulders at 1000 cm^{-1}, 840 and 700 cm^{-1} associated with $Nb - O$ stretching vibrations, which indicate the presence of Nb oxides. Thus, the FTIR results show that as the amount of oxygen increases, a change in coating composition occurs, going from nitride-type to Nb_2O_5-type.

These results show that beyond a clear change of signal types, a strong coherence with the composition evolutions and the thermodynamics data is observed. Moreover, this behaviour is also consistent with the previous multilayer effect observed in these films [15]. As the duty cycle increases, the thickness of the oxide-rich layer becomes dominant thus giving rise to clearer FTIR oxide bands.

Thermal behaviour

Composition variations

Taking into account that a high oxidation resistance of a material determines its stability, functionality and long term performance in an oxidizing working environment, we carried out oxidation experiments in-air. The evolution of the oxidation pro-

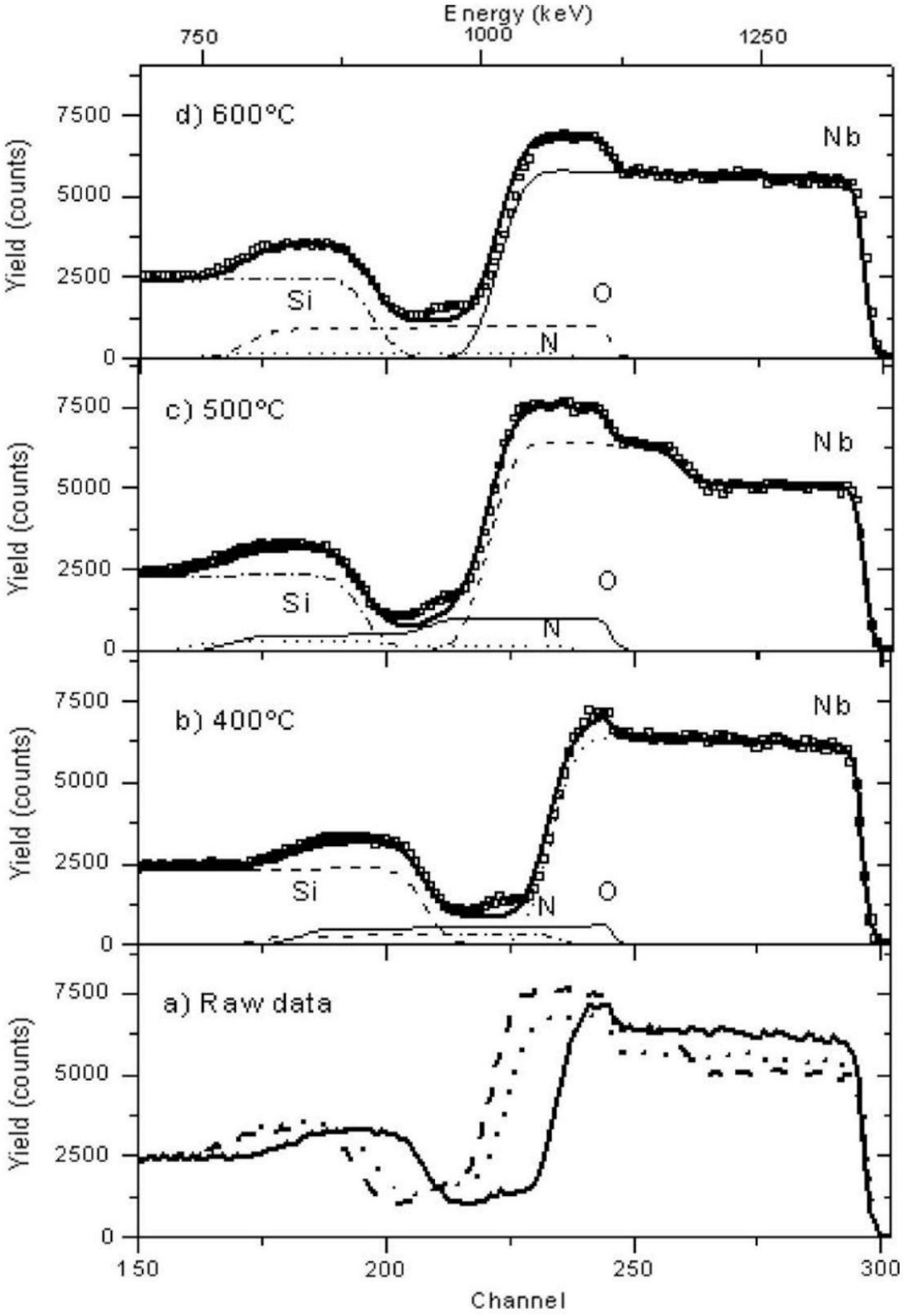
Energy (keV)
750
1000
1250
d) 600°C
c) 500°C
b) 400°C
a) Raw data
Nb
Si
O
N
Yield (counts)
7500
5000
2500
0
150
200
250
300
Channel

Fig. 4. RBS spectra for the annealed NbON layer grown with $\alpha = 0.6$ (a) and the simulation results after annealing at 400°C (b) 500°C (c) and 600°C (d). cess was followed by RBS and XRD after each annealing step. Fig. 3 is a typical example of the RBS measurements. In this case the spectra show the results obtained for the as deposited samples obtained with a $1.4MeV\,^{1}H^{+}$beam and a target tilt of 30°.

Increasing the value of the duty cycle leads to a decrease of the height of the Nb signal indicating a lower incorporation of Nb in the films. A detailed analysis of the data using the NDF code allows us to obtain the concentration profiles of the individual elements in the film as shown in Fig. 3(b)-(d). In all the cases the concentration of all the elements (indicated in Fig. 1) remains constant through the entire film thickness (within the depth resolution of RBS). The oxidation process was found to be similar for all the samples during the isochronal annealing. As an example in Fig. 4 we show the RBS data for the sample with a duty cycle of $\alpha = 0.6$.

A two-layer macro-structure composed of an oxide-rich surface film (oxide layer) on the top of the deposited layer can clearly be seen at 500°C (Fig. 4(c)). The simulations indicate an increase of the oxygen content accompanied by a depletion of nitrogen. At 600°C the original film is fully oxidized. These findings are summarized in Fig. 5 (this figure shows the composition of the surface

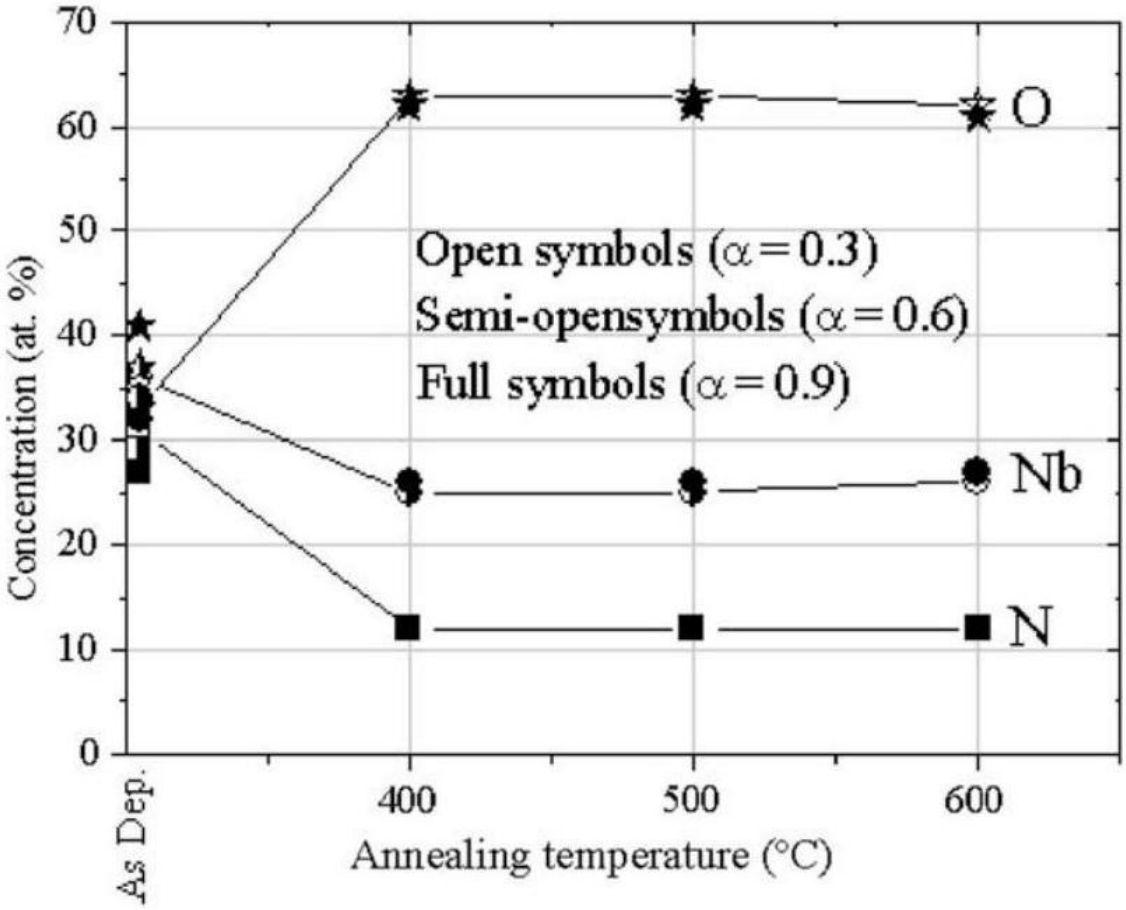

Fig. 5. Composition of surface layers of $NbO_x N_y$ samples prepared with different duty cycles and annealed at temperatures of $400°C, 500°C$ and $600°C$.

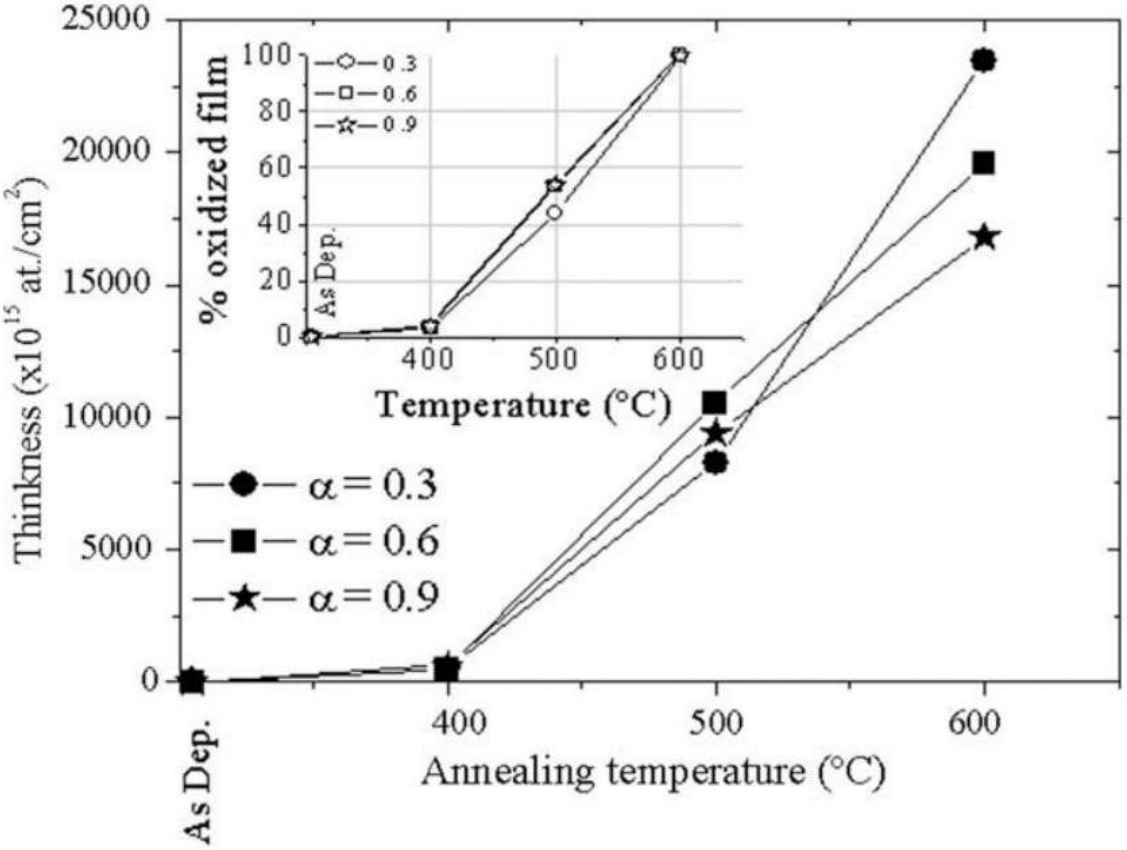

Fig. 6. Thickness of the oxidized layers as a function of annealing temperature for the three samples prepared with different duty cycles. In the upper left insert, the plot represents the percentage of oxidized film as a function of annealing temperature for the three different duty cycles.
layer, whereas Figs. 3 and 4 contains the composition of the whole film).

The first important note about the results plotted in Fig. 5 is the significant similarity in the oxide layers that are formed for the different temperatures. Although with different thicknesses (see Fig. 6), all samples seem to develop the same chemical composition of the oxide-oxynitride surface layer, whose composition is about $NbO_{2.4} N_{0.5}$ (or $Nb_2O_{4.8} N$). The composition profiles reveal an almost homogeneous in-depth composition for all samples at all annealing temperatures, revealing that no protective layers are formed. This suggests that the oxidation kinetics of the coatings is diffusion limited, indicating that the inward diffusion of O^{2-} spe-

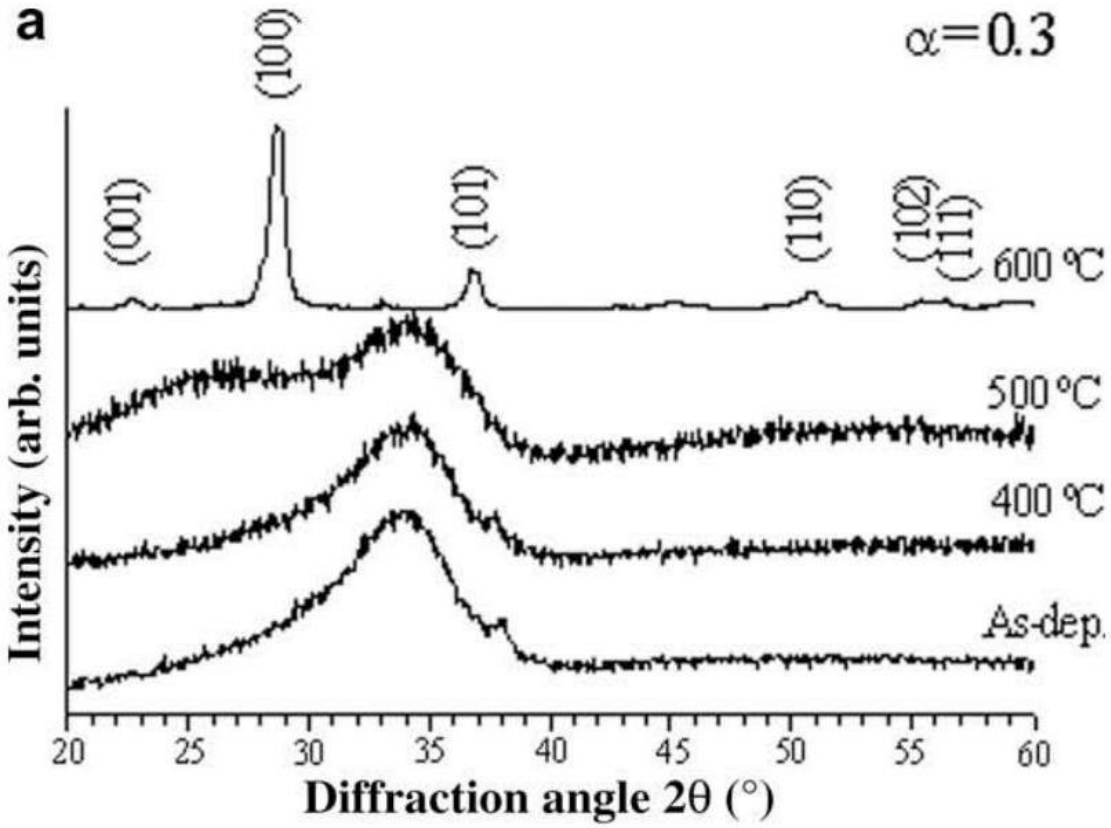
a
α=0.3
(001)
(100)
(101)
(110)
(102)
(111)
600 °C
500 °C
400 °C
As-dep.
Intensity (arb. units)
20
25
30
35
40
45
50
55
60
Diffraction angle 2θ (°)

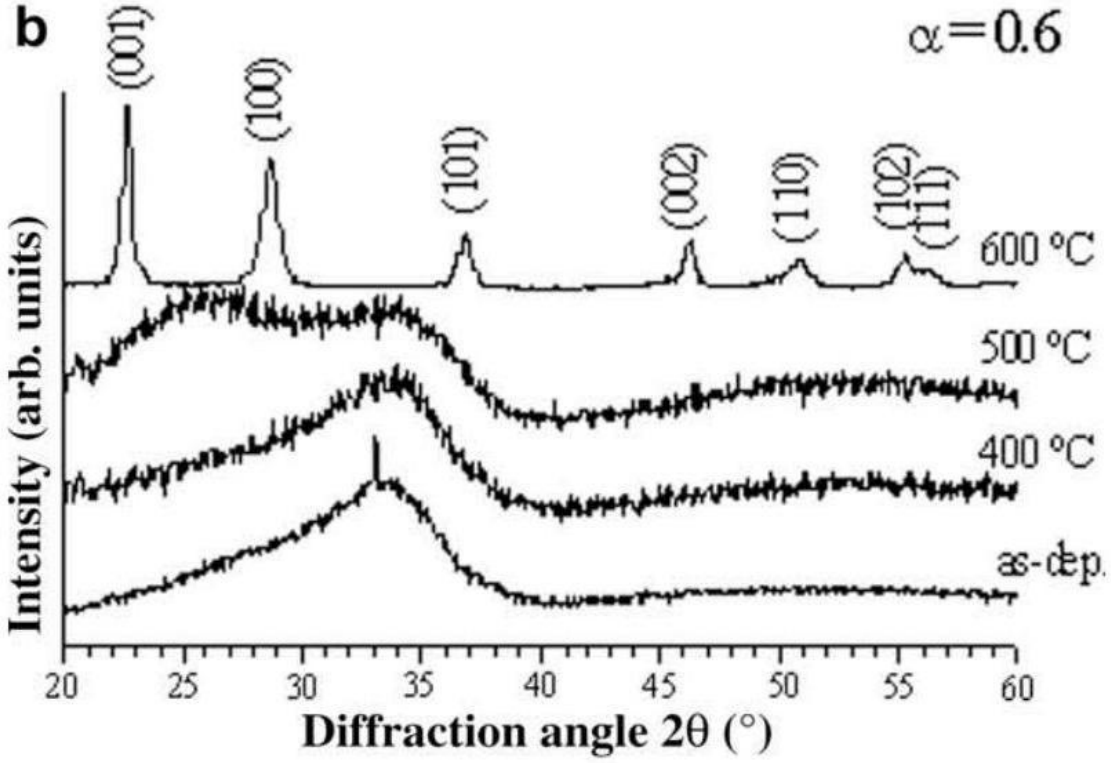
b
α=0.6
(001)
(100)
(101)
(002)
(110)
(102)
(111)
600 °C
500 °C
400 °C
as-dep.
Intensity (arb. units)
20
25
30
35
40
45
50
55
60
Diffraction angle 2θ (°)

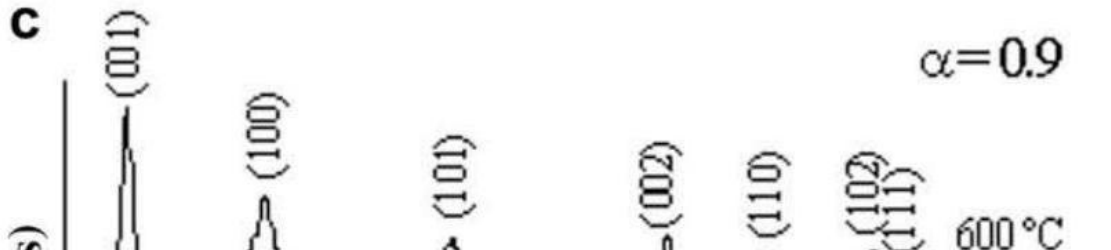
c
α=0.9
(001)
(100)
(101)
(002)
(110)
(102)
(111)
600 °C

Fig. 7. XRD analysis for the as-deposited and annealed samples at 400°C, 500°C and 600°C, prepared with different duty cycles.
cies through the already grown oxide is probably the rate limiting process. As already mentioned in the introduction, diffusion of oxygen in Nb_2O_5 is expected to occur along the relatively open channels between the $Nb-O$ octaeders [13].

For all films, at 400°C, a very thin oxide layer starts to form at the surface with enhanced O concentration (this can be seen from the details of the RBS simulation, namely in the shape of the Nb edge and in the surface O signal, Fig. 4). The apparent reduction of both Nb and N concentrations in Fig. 5 is only the reflex of an increasing amount of oxygen present in the films, i.e. the total NbON layer is growing - leading to a thicker coating, which in fact increases with increasing annealing temperature. At 500°C, this oxide layer becomes thicker, encompassing about half the film thickness. As mentioned before the simulations reveal that the increase of the O in the oxide scale is accompanied by a reduction of both Nb and N . The N concentration in the oxide layer is close to the detection limits, which makes it very difficult to give any conclusion about its presence. At 600°C, the process is finished and a single oxide layer is formed with reduced Nb and increased O concentration. Again, we are unable to tell about the presence of N . Fig. 6 shows a detail of the evolution of the oxide film thickness. Again, and similarly to what has been observed for the composition, the thickness of the oxide layers do not vary significantly with the duty cycle, as well as the percentage of the oxidized film.

Structural changes

To follow the important changes with annealing temperature, extensive XRD experiments were conducted. Fig. 7 shows the results obtained for the three sets of samples (as-deposited and annealed samples).

The XRD experiments seem to clearly evidence the first observations. In fact, there is a evident and progressive change from a roughly X-ray amorphous nature of the films to crystallized films at 600°C. In spite of the already mentioned composition differences in the as-deposited samples, the phase evolutions are very similar for all coatings, showing that a clear crystallization is occurring at 600°C. The different diffraction peaks can be indexed to a Nb_2O_5-type structure, which in fact is consistent with the composition results that revealed a $Nb_2O_{4.8}$ N-type composition for the oxide layer. Nevertheless, it is important to emphasize the amount of nitrogen present in the oxide layer ($\sim 12at.\%$), which could be either: (a) dispersed within the oxide matrix, (b) located at the grain boundaries in the form of amorphous nitride-based compound or (c) existing as a second phase besides Nb_2O_5 (e.g. nanosized NbN crystals or amorphous $Nb-O-N$).

The crystallization at 600 °C of niobium oxide (Nb_2O_5) was also reported by Rosenfeld et al. for thermal treatments in synthetic air [20,21]. Other authors reported a crystallization temperature of 500 °C for Nb_2O_5 when annealing in Ar atmospheres [22], developing the same crystalline Nb_2O_5-type structure.

Conclusions

The structural and compositional changes of NbON multilayers during oxidation in air were studied by Rutherford backscattering spectrometry, X-ray diffraction and infrared spectroscopy. The asgrown films showed a

homogeneous composition through all the entire thickness (due to insufficient resolution of these methods) and an increase of the Nb concentration for higher O_2 flow rates, i.e. higher duty cycles. The as-deposited films are mostly X-ray amorphous and crystallize in the form of Nb_2O_5 after annealing at 600°C. At this temperature all the films became completely oxidized and the nitrogen is depleted from the oxide layer. The oxidation kinetics of the films was determined to be diffusion limited, indicating that it is the oxygen diffusion through the oxide scale which limits the process.

Acknowledgements

This work was supported by the European Community under Grant No. NMP3-CT-2003-505948 (Project acronym "HARDECOAT"). The authors J.M. Chappé and P. Carvalho also thank "Fundação para a Ciência e Tecnologia" of Portugal for the postdoctorate grant SFRH/BPD/27114/2006 and Ph.D. Grant SFRH/BD/ 31907/2006, respectively.

References

[1] P. Carvalho, F. Vaz, L. Rebouta, L. Cunha, C.J. Tavares, C. Moura, E. Alves, A. Cavaleiro, P. Goudeau, E. Le Bourhis, J.P. Rivière, J.F. Pierson, O. Banakh, J. Appl. Phys. 98 (2005) 023715.
[2] M. Lazarov, P. Raths, H. Metzger, W. Spirkl, J. Appl. Phys. 77 (1995) 2133.
[3] S. Collard, H. Kupfer, G. Hecht, W. Hoyer, H. Moussaoui, Surf. Coat. Technol. 112 (1999) 181.
[4] K.J. Lee, D.J. Kim, US Patent US2002019110, 2002.
[5] J. Probst, U. Gbureck, R. Thull, Surf. Coat. Technol. 148 (2001) 226.
[6] F. Richard, F. Hickernell, F. Cho, US Patent US4701008, 1987.
[7] T. Savisalo, D.B. Lewis, P.Eh. Hovsepian, Surf. Coat. Technol. 200 (2006) 2731.
[8] R. Brayner, G. Djéga-Mariadassou, G. Marques da Cruz, J.A. Jorge Rodrigues, Catal. Today 57 (2000) 225.
[9] H.S. Kim, C.H. Shin, G. Bugli, M. Bureau-Tardy, G. Djega-Mariadassou, Appl. Catal. A: General 119 (1994) 223.
[10] M. Fenker, H. Kappl, K. Petrikowski, R. Bretzler, Surf. Coat. Technol. 200 (2005) 1356.
[11] M. Fenker, H. Kappl, O. Banakh, N. Martin, J.F. Pierson, Surf. Coat. Technol. 201 (2006) 4152.
[12] J.M. Chappé, P. Carvalho, S. Lanceros-Mendez, M.I. Vasilevskiy, F. Vaz, A.V. Machado, M. Fenker, H. Kappl, N.M.G. Parreira, A. Cavaleiro, E. Alves, Surf. Coat. Technol. 202 (2008) 2363.
[13] Gmelins Handbuch der Anorganischen Chemie, eighth ed., Niobium - Part B1, Verlag Chemie GmbH, Weinheim/Bergstr., 1970.
[14] A.R. Ramos, A. Paúl, L. Rijniers, M.F. da Silva, J.C. Soares, Nucl. Instr. and Meth. B 190 (2002) 95.
[15] M. Fenker, H. Kappl, C.S. Sandu, Surf. Coat. Technol. 202 (2008) 2358.
[16] M. Benkahoul, C.S. Sandu, N. Tabet, M. Parlinska-Wojtan, A. Karimia, F. Lévy, Surf. Coat. Technol. 188-189 (2004) 435.
[17] A. Pawlicka, M. Atik, M.A. Aegerter, Thin Solid Films 301 (1997) 236.
[18] A. Jasik, R. Wojcieszak, S. Monteverdi, M. Ziolek, M.M. Bettahar, J. Mole. Catal. A: Chem. 242 (2005) 81.
[19] H. Szymanowski, O. Zabeida, J.E. Klemberg-Sapieha, L. Martinu, J. Vac. Sci. Technol.

A 23 (2) (2005) 241.
[20] D. Rosenfeld, R. Sanjinès, F. Lévy, P.A. Buffat, V. Demarne, A. Grisel, J. Vac. Sci. Technol. A12 (1994) 135.
[21] F. Lai, M. Li, H. Wang, H. Hu, X. Wang, J.G. Hou, Y. Song, Y. Jiang, Thin Solid Films 488 (2005) 314.
[22] S. Venkataraj, R. Drese, Ch. Liesch, O. Kappertz, R. Jayavel, M. Wuttig, J. Appl. Phys. 91 (8) (2002) 486.